

# Photoconductive Enhancement Effects of Graphene Quantum Dots on ZnO Nanoparticle Photodetectors

Dali Shao and Shayla Sawyer

Electrical, Computer, and Systems Engineering Department  
Rensselaer Polytechnic Institute  
Troy, NY 12180, USA  
shaod@rpi.edu

Tao Hu, Mingpeng Yu and Jie Lian

Mechanical, Aerospace & Nuclear Engineering Department  
Rensselaer Polytechnic Institute  
Troy, NY 12180, USA

**Abstract**—Graphene quantum dots (GQDs) are a new class of zero dimensional carbon materials and have fascinating optical and electric properties. Many different methods for GQDs synthesis have been reported and GQDs have been proved very promising for biomedical imaging and photovoltaics applications. In order to further investigate the application of GQDs, here we report solution processable ultraviolet (UV) photodetector fabricated from ZnO nanoparticles (NPs) and from GQDs synthesized from hydrothermal method. The photodetector employing GQDs showed enhanced photoresponsivity and improved transient response. These improvements are explained by referring to the energy band diagram of the interfacial region of ZnO NPs and GQDs. The GQDs in this work demonstrated high potential for solution processable optoelectronics.

**Index Terms**—Graphene quantum dots, UV photodetector, ZnO nanoparticles

## I. INTRODUCTION

As a new class of zero dimensional carbon materials, GQDs can overcome the extremely poor solubility and strong tendency to aggregation of the conventional graphene sheets. Moreover, GQDs' high specific surface area for a large interface, high carrier mobility and tunable energy gap should have great potential for optoelectronics applications [1-7]. Recent studies have proved GQDs to be very promising for high contrast biomedical imaging and photovoltaics [8-10]. However, GQDs for photodetector applications haven't been studied yet. In this work, we fabricated GQDs/PVA-ZnO UV photodetector as an example to demonstrate GQDs' high potential in this field. According to best of our knowledge, this is the first time for GQDs be used for solution processable UV photodetector applications.

## II. EXPERIMENTAL DETAILS

Graphene quantum dots were synthesized based on hydrothermal route [11]. Briefly, Graphene sheets (GS) were oxidized in concentrated  $H_2SO_4$  and  $HNO_3$  (volume ratio: 1:3) for 20 h under ultrasonication (500 W, 40 kHz). The mixture was then diluted with deionized (DI) water and filtered through a 0.22 micrometer membrane. Oxidized GSs were dissolved in DI water with pH tuned to 8 with  $NH_3 \cdot H_2O$  and hydrothermally

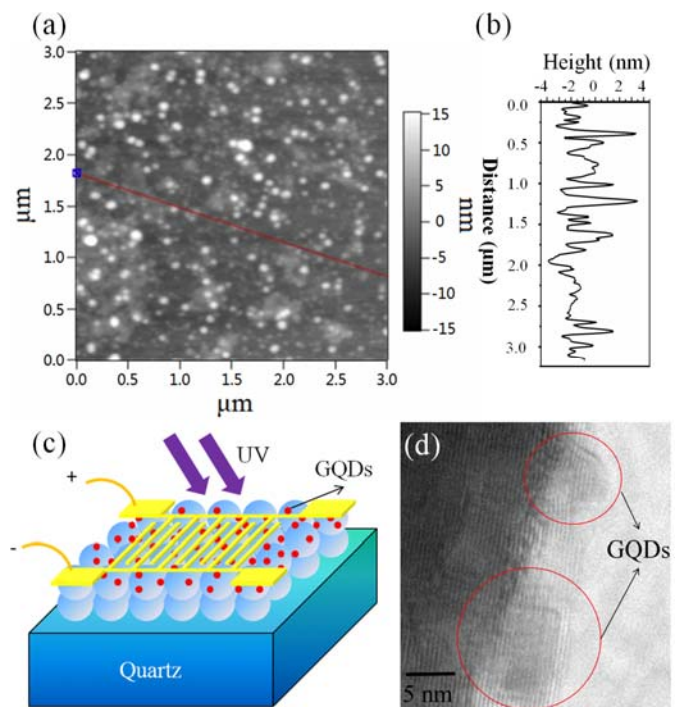


Figure 1. (a) AFM image of the as-prepared GQDs. (b) Height distribution profile of the GQDs along the red line in (a). (c) 3D view of the fabricated UV photodetector. (d) High resolution TEM image of the GQDs deposited onto the ZnO NPs surface.

treated in a Teflon-lined Parr autoclave and heated at  $200^{\circ}C$  for 10h. After cooling down to room temperature, the solution was filtered through a 0.22 micrometer membrane. A light-yellow solution containing fluorescent GQDs was obtained after a process of dialysation. The fabricated GQDs can be retained stably in water for several months without any change.

The UV photodetectors were fabricated from high purity ZnO NPs with sizes ranging from 100-150 nm. These ZnO NPs were synthesized using low temperature top-down wet-chemical etching method and then surface treated with PVA solutions (1% in weight in water). The PVA can provide surface passivation for metal oxide nanoparticles and the

details have been reported in our previous works [12-13]. The PVA coated ZnO nanoparticles were centrifuged and dispersed

view of the fabricated UV photodetector is shown in Figure 1 (c). Figure 1 (d) present a high resolution transmission electron

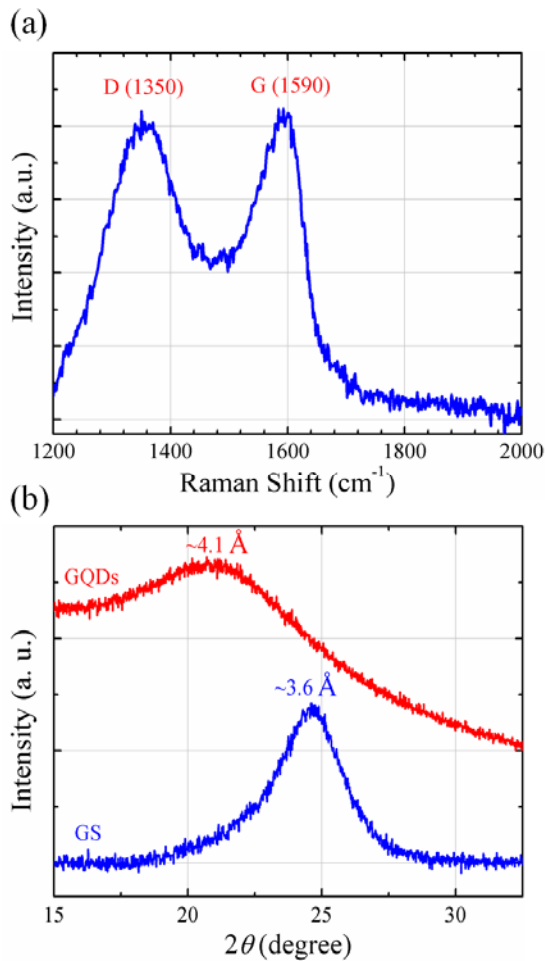


Figure 2. (a) Raman spectra of the GQDs. (b) XRD spectra of the original GS and GQDs.

in ethanol to form a suspension with concentration at 30 mg/ml. The solution was then spin-coated onto quartz substrate and annealed in air at 100°C for 5 min. Then, the yellow solution contain GQDs was deposited onto PVA-ZnO NPs thin film using a simple drop casting method. Aluminum (Al) contacts were deposited on top of the samples using E-beam evaporation through a shadow mask. The Al contacts had a thickness of about 250 nm and were patterned as interdigitated fingers. The inter-electrode distance (diagonal) is approximately 4mm. Finally, the photodetector was packaged and wire bonded using Epo-Tek H20E conductive epoxy.

### III. RESULTS AND DISCUSSIONS

The atomic force microscope image of the as-prepared GQDs and the height distribution profile are shown in Figure 1 (a) and (b), respectively. The diameters of the GQDs are estimated to be around 10 nm in average. The topographic heights of the GQDs are mostly between 3 and 4 nm, corresponding to 2 to 4 graphene layers. The three dimensional

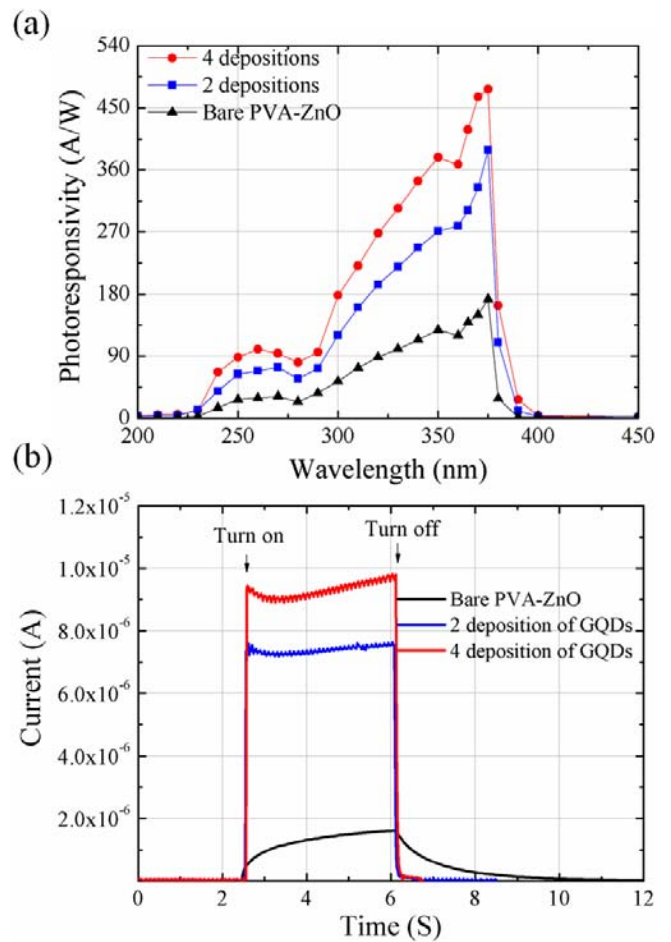


Figure 3. (a) Photoresponsivity spectra and (b) transient response of the UV photodetectors with varying deposition times of the GQDs.

microscopy image of the GQDs deposited on the ZnO NPs surface.

The major Raman features are shown in Figure 2 (a), where the D band at around 1350  $\text{cm}^{-1}$  and the G band at around 1590  $\text{cm}^{-1}$  were observed. The relative intensity of the “disorder” D-band and the crystalline G-band ( $I_D / I_G$ ) for as produced GQDs in this work is around 1, which is lower than the value calculated in reference 8 using the same method, indicates a better quality of the as-prepared GQDs. The X-ray diffraction (XRD) profiles for the as-prepared GQDs and the GS are presented in Figure 2 (b). The GS have a broad (002) peak centered at around 24.6 degrees, corresponding to an interlayer spacing of 0.36 nm. The XRD peak for GQDs shifted to a lower degree (21.5 degrees, 0.41 nm) compared with the GS, indicating that GQDs had a bigger interlayer spacing than that of the original GS. This result could be attributed to the oxygen-containing groups introduced in the exfoliation and oxidation of GS, which increased the interlayer distance.

The responsivity of the devices (shown in Figure 3 (a)), defined as photocurrent per unit of incident optical power, was

measured by Shimadzu UV-Vis 2550 spectrophotometer with a deuterium lamp (190-390 nm) and a halogen lamp (280-1100

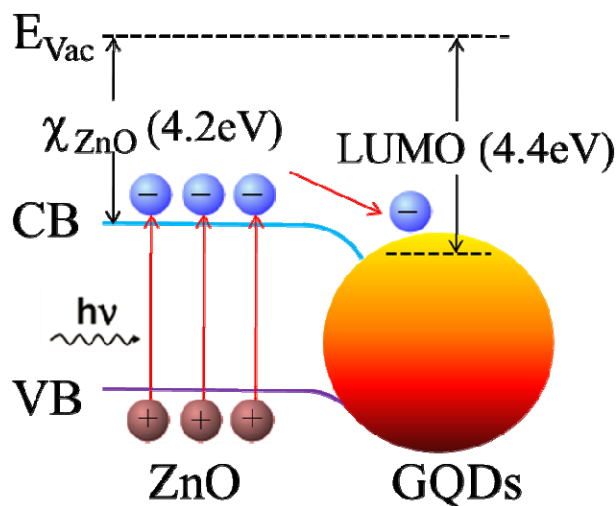


Figure 4. Energy band diagram and carrier transport mechanism in the interfacial region of GQDs and ZnO NPs.

nm). Three devices with varying deposition times of the GQDs were measured. The photoresponsivity spectra observed for these samples have peaks located at 375 nm, which are due to near band edge (NBE) transitions in ZnO. Quite promising, the photoresponsivity of the UV photodetector with two depositions of GQDs was more than doubled compared to the reference sample without the GQDs. The UV photodetector with four depositions of GQDs showed even higher photoresponsivity.

Not only the photoresponsivity spectra were enhanced, the UV photodetectors with depositions of GQDs also present huge improvement in the transient response (shown in Figure 3 (b)). Note that the transient responses of the UV photodetectors were measured by turning on and off a 335 nm UV LED. For the two UV photodetectors with depositions of GQDs, the rise time and fall time are less than 0.06 s and 0.08 s, respectively. This is much faster than the reference sample, whose rise time and fall time are both longer than 3 seconds. The enhanced photoresponsivity and improved transient photoresponse can be understood by referring the energy band diagram and carrier transportation process of the GQDs/PVA-ZnO composite structure, as shown in Figure 4.

The electron affinity for ZnO is around 4.2 eV below the vacuum level [14]. The lowest unoccupied molecule orbital of GQDs was measured using electrochemical method [8] and was estimated to be around 4.4 eV below the vacuum level. Thus, when ZnO contact with the GQDs, it is energetically favorable for the electron to transfer from the ZnO to the GQDs. With UV illumination, the photogenerated electrons reach the ZnO conduction band and then transfers to the GQDs. GQDs effectively afford exciton separation interfaces and carrier transporting pathways, which led to the dramatic increase of photocurrent [8]. GQDs have high electron mobility, which accordingly are conducive to electron transport in the active

film. Therefore, charge separation could not only effectively take place in the PVA-ZnO device, but also the transport of charge carriers could be enhanced significantly.

#### IV. CONCLUSION

In conclusion, solution processable GQDs were fabricated using hydrothermal process. The UV photodetectors fabricated from these GQDs and PVA-ZnO shows enhanced photoresponsivity spectra and greatly improved transient photoresponse. These improvements are attributed to enhanced carrier separation and more efficient carrier transportation process by employing the GQDs, proving one of promising applications of GQDs in optoelectronics.

#### ACKNOWLEDGMENT

The authors gratefully acknowledge support from National Security Technologies through NSF Industry/University Cooperative Research Center Connection One. The authors also acknowledge the National Science Foundation Smart Lighting Engineering Research Center (EEC-0812056) and a NSF career award DMR 1151028. The author Mingpeng Yu thanks for the financial support from China Scholarship Council (CSC File No.2010646040).

#### REFERENCES

- [1] K. Geim, Science, "Graphene status and prospects," vol. 324, pp.1530-1534, 2009.
- [2] S. Watcharotone, D. A. Dikin, S. Stankovich, R. Piner, I. Jung, G. H. B. Dommett, G. Evmenenko, S. E. Wu, S. F. Chen, C. P. Liu, S. T. Nguyen, R. S. Ruoff, "Graphene-silica composite thin films as transparent conductors," Nano Lett. vol 7, pp. 1888-1892, 2007.
- [3] L. A. Ponomarenko, F. Schedin, M. I. Katsnelson, R. Yang, E. W. Hill, K. S. Novoselov, A. K. Geim, "Chaotic dirac billiard in graphene quantum dots," Science vol. 320, pp. 356-358, 2008.
- [4] X. Wang, L. Zhi, K. Mullen, "Transparent, conductive graphene electrodes for dye-sensitized solar cells," Nano Lett. vol. 8, pp. 323-327, 2008.
- [5] C. O. Girit , J. C. Meyer , R. Erni , M. D. Rossell , C. Kisielowski , L. Yang , C. H. Park , M. F. Crommie , M. L. Cohen , S. G. Louie , A. Zettl, "Graphene at the edge: stability and dynamics," Science vol. 323, pp. 1705-1708 2009.
- [6] A. K. Geim, K. S. Novoselov, "The rise of graphene," Nat. Mater. vol. 6, pp. 183-191, 2007.
- [7] M. Choucair, P. Thordarson, J. A. Stride, "Gram-scale production of graphene based on solvothermal synthesis and sonication," Nat. Nanotechnol. vol 4, pp. 30-33, 2009.
- [8] Y. Li , Y. Hu , Y. Zhao , G. Shi , L. Deng , Y. Hou and L. Qu, "An electrochemical avenue to green-luminescent graphene quantum dots as potential electron-acceptors for photovoltaics," Adv. Mater. vol. 23, pp. 776-780, 2011.
- [9] J. Peng, W. Gao, B. K. Gupta, Z. Liu, R. Romero-Aburto, L. Ge, L. Song, L. B. Alemany, X. Zhan, G. Gao, S. A. Vithayathil, B. A. Kaiparettu, A. A. Marti, T. Hayashi, J.-J. Zhu, and P. M. Ajayan, "Graphene quantum dots derived

- from carbon fibers,” Nano Lett. vol. 12, pp. 844-849, 2012.
- [10] Z. F. Liu , Q. Liu , Y. Huang , Y. F. Ma , S. G. Yin , X. Y. Zhang , W. Sun , Y. S. Chen, “Organic photovoltaic devices based on a novel acceptor material: graphene,” Adv. Mater. vol. 20, pp. 3924-3930, 2008.
- [11] D. Pan, J. Zhang, Z. Li and M. Wu, “Hydrothermal Route for Cutting Graphene Sheets into Blue-Luminescent Graphene Quantum Dots,” Adv. Mater. vol. 22, pp. 734-748, 2010.
- [12] D. Shao, L. Qin and S. Sawyer, “High Responsivity, Bandpass Near-UV Photodetector Fabricated From PVA-In<sub>2</sub>O<sub>3</sub> Nanoparticles on a GaN Substrate,” IEEE Photonics J. vol. 4, pp. 715-720, 2012.
- [13] L. Qin, C. Shing, S. Sawyer, and P. S. Dutta, “Enhanced UV sensitivity of ZnO nanoparticle photoconductors by surface passivation,” Opt. Mater. vol. 33, pp. 359-362, 2011.
- [14] L. J. Brillson and Y. Lu, “ZnO Schottky barriers and Ohmic contacts,” J. Appl. Phys. vol. 109, pp. 121301 1-33, 2011.